Cell Transplantation
2018, Vol. 27(10) 1434–1450

DOI: 10.1177/0963689718792203
journals.sagepub.com/home/cll
SAGE

Growth Factor-Mediated Tenogenic Induction of Multipotent Mesenchymal Stromal Cells Is Altered by the Microenvironment of Tendon Matrix

Susanne Pauline Roth[1,2], Susanna Schubert[2,3], Patrick Scheibe[2], Claudia Groß[2], Walter Brehm[1], and Janina Burk[1,3]

Abstract

Age-related degenerative changes in tendon tissue represent a common cause for acute tendon pathologies. Although the regenerative potential of multipotent mesenchymal stromal cells (MSC) was reported to restore functionality in injured tendon tissue, cellular mechanisms of action remain partly unclear. Potential tenogenic differentiation of applied MSC is affected by various intrinsic and extrinsic factors. The current study presents an *in vitro* model to evaluate the combined extrinsic effects of decellularized equine tendon matrix, transforming growth factor beta 3 (TGFβ3) and bone morphogenetic protein 12 (BMP12) on the tenogenic fate of equine adipose tissue-derived MSC. Monolayer MSC cultures supplemented with TGFβ3 and BMP12 as well as MSC cultured on tendon matrix scaffolds preloaded with the growth factors were incubated for 3 and 5 days. Histological evaluation and real time reverse transcription polymerase chain reaction (RT-PCR) revealed that growth factor-mediated tenogenic induction of MSC was modified by the conditions of the surrounding microenvironment. While the gene expression pattern in monolayer cultures supplemented with TGFβ3 or TGFβ3 and BMP12 revealed an upregulation for collagen 1A2, collagen 3A1, tenascin c, scleraxis and mohawk ($p < 0.05$), the presence of tendon matrix led to an upregulation of decorin and osteopontin as well as to a downregulation of smad8 ($p < 0.05$). Preloading of scaffolds with either TGFβ3, or with TGFβ3 and BMP12 promoted a tenocyte-like phenotype and improved cell alignment. Furthermore, gene expression in scaffold culture was modulated by TGFβ3 and/or BMP12, with downregulation of collagen 1A2, collagen 3A1, decorin, scleraxis, smad8 and osteopontin, whereas gene expression of tenascin c was increased. This study shows that growth factor-induced tenogenic differentiation of equine MSC is markedly altered by topographical constraints of decellularized tendon tissue *in vitro*. While TGFβ3 represents an effective mediator for tenogenic induction, the role of BMP12 in tenogenesis may be of modulatory character and needs further evaluation.

Keywords

cell therapy, tissue engineering, tendon, horse, multipotent mesenchymal stromal cells (MSC), transforming growth factor beta 3 (TGFβ3)

Introduction

Tendon pathologies represent frequently occurring long-term musculoskeletal disorders in the contemporary population structure[1,2]. Epidemiological studies have shown a clear link between age as predisposing factor and an increased incidence of tendon pathologies[3,4]. Natural ageing processes result in chronically degenerated tendon tissue, which is prone to acute trauma[5]. Within recent decades, the high number of affected patients, the limited regenerative capacity of tendon tissue and the ineffectiveness of conventional treatment options have encouraged regenerative approaches

[1] Faculty of Veterinary Medicine, Veterinary Teaching Hospital Department for Horses, Universität Leipzig, Germany
[2] Saxonian Incubator for Clinical Translation, Universität Leipzig, Germany
[3] Faculty of Veterinary Medicine, Institute of Veterinary Physiology, Universität Leipzig, Germany

Submitted: December 19, 2017. Revised: June 25, 2018. Accepted: July 6, 2018.

Corresponding Author:
Susanne Pauline Roth, Universität Leipzig, Saxonian Incubator for Clinical Translation, Philipp-Rosenthal-Strasse 55, D-04103 Leipzig, Germany.
Email: susanne.roth@uni-leipzig.de

to restore functionality in injured tendon tissue. Local injections of multipotent mesenchymal stromal cells (MSC) have been pioneered with promising results, especially in equine patients[6–9]. However, the cellular mechanisms of action by which applied MSC influence repair and regeneration in tendon tissue have not been elucidated completely. Besides various paracrine effects of MSC, it is assumed that MSC-mediated therapeutic effects are due in part to cell differentiation, which results not only in the replacement of tenocytes, but also in the production and modulation of tendon extracellular matrix (ECM)[9–11]. The latter includes collagen 1A2 as most abundant extracellular protein, playing a pivotal role in a functional tendon tissue architecture. Furthermore, ECM components like the small leucine rich proteoglycan decorin influence not only the collagen fibril structure, but also regulate cell proliferation and stimulate immune responses, thereby entailing additional immunomodulatory effects of MSC[12,13].

However, molecular cascades that lead to tenogenic differentiation of MSC remain partly unclear[1]. A unique composition of conserved ECM components and an accurately timed deposition and presentation of soluble factors maintain the sensitive balance of tissue homoeostasis including cell differentiation[14–16]. Correspondingly, reported tenogenic factors include specific scaffold biomaterials as well as growth factors, particularly transforming growth factor beta 3 (TGFβ3) and bone morphogenetic protein 12 (BMP12 / GDF7 / CDMP 3)[17].

Tendon tissue has one of the highest matrix-to-cell-ratios, thus structural and regulatory molecules of tendon ECM are of major importance for full tissue operability. With regard to scaffold biomaterials, it was shown that providing topographical as well as biochemical cues is of importance for tenogenic differentiation. Artificial scaffolds presenting an aligned fibre pattern promoted not only tenogenesis, but also impaired osteogenetic induction compared with scaffolds with a randomly oriented fibre pattern[18,19]. This indicates the importance of a scaffold architecture resembling the hierarchically structured tendon ECM as an influencing factor for tenogenesis. Furthermore, the soluble urea extracted fraction of tendon ECM stimulated tenogenesis in human adipose stem cells, suggesting that the biochemical ECM composition equally influences cell differentiation[20]. Both tendon ECM architecture, as well as biochemical composition, are maintained in decellularized tendon matrix, which in consequence favourably mimics tendon microenvironment. When bone marrow derived MSC of rats were cultured onto decellularized Achilles tendon slices, an increased gene expression of tendon related genes like tenomodulin and thrombospondin 4 was observed[21]. Moreover, culture on decellularized tendon scaffolds altered the expression of tendon marker proteins in equine adipose tissue derived MSC[10].

Both TGFβ3 and BMP12 are members of the TGFβ-superfamily and represent prototypes of multifunctional, contextually acting growth factors with a major switching function in the regulation of development, disease, and repair[22]. In developmental studies, TGFβ3 was found to be present during tendon tissue morphogenesis in chickens[23]. Studies in a rat model of tendon healing revealed an interaction between the TGFβ isoforms concerning the regulation of collagen synthesis and show further a complex regulatory system for the spatial distribution of the TGFβ isoforms and their receptors in healing tendon tissue[24]. An exogenous supplementation of TGFβ3 led to an upregulation of tendon associated genes in cell cultures of different cell types[24–26]. BMPs were originally named for their ability to induce ectopic bone formation[27,28]. However, BMP12 represents an exception to this and rather has a distinctive capacity to induce tenogenic differentiation[29]. BMP12 gene transfection revealed upregulated expression of collagen 1 and increased expression of intracellular tendon associated genes[30,31]. Furthermore, exogenous BMP12 supplementation induced tenogenic differentiation in MSC from diverse sources in monolayer cultures as well as in collagen scaffold cultures, which additionally improved tendon healing in rat calcaneal tendon defects *in vivo*[32–34]. Direct BMP12 injections in rat Achilles tendon defects showed a significant dose-related increase in strength and stiffness 8 days after application[35].

Besides individual effects of TGFβ3 and BMP12, a complex crosstalk between TGFβ and BMP signalling has been suggested[36]. Furthermore, due to their context sensitive activity, it can be assumed that their effects depend on the microenvironment, in which tendon ECM or scaffold materials would play a major role. Correspondingly, a recent study showed synergistic effects of both pulverised tendon ECM as well as aligned electrospun scaffolds with TGFβ3[37]. However, to the author's knowledge, TGFβ3- or BMP12-induced tenogenic differentiation has not been investigated in the microenvironment of preserved natural tendon ECM.

Therefore, this study aimed to investigate the combined effects of decellularized tendon scaffolds, TGFβ3 and BMP12. To allow an interaction of the growth factors with the prepared tendon ECM-based scaffolds, a newly established technique of preloading them to the scaffold prior to cell seeding was used for studying the combined effects. Our hypotheses were that TGFβ3 and BMP12 would synergistically induce tenogenic differentiation, and that this effect would be supported by the tendon ECM-based microenvironment.

Materials and Methods

Study Design

Adipose tissue-derived MSC ($n = 7$ biological replicates) were cultured as monolayers as well as on scaffolds obtained from decellularized tendon tissue. Scaffolds were preloaded, and medium for monolayer cultures was supplemented with TGFβ3, BMP12 or a combination of TGFβ3 and BMP12. The respective controls were prepared accordingly but without addition of growth factors. Samples were incubated until day 3 and day 5 when the following parameters were

assessed to evaluate tenogenic differentiation: 1) macroscopic scaffold morphology, 2) cell distribution and integration as determined by histological evaluation, 3) LIVE/DEAD® staining as well as 4) gene expression of tendon extracellular matrix molecules and intracellular tendon markers. The two latter criteria were also applied to growth factor treated monolayer cultures.

Mesenchymal Stromal Cell Recovery

MSC were recovered from the subcutaneous adipose tissue of seven healthy horses aged 1–5 years, which were euthanized for reasons unrelated to the present study. After the equine adipose tissue was collected under sterile conditions, it was minced and subjected to enzymatic digestion by collagenase I solution (0.8 mg/ml; Thermo Fisher Scientific/Life Technologies, Karlsruhe, Germany) at 37°C for 4 h. For further cultivation, the released cell fraction was suspended in standard cell culture medium [Dulbecco's modified Eagle medium 1 g glucose/L (Gibco® by Life Technologies, Karlsruhe, Germany) supplemented with 10% fetal bovine serum (FBS; Gibco® by Life Technologies, Karlsruhe, Germany), 1% penicillin streptomycin (Sigma Aldrich, St. Louis, MO, USA) and 0.1% gentamycin (Carl Roth, Karlsruhe, Germany)] and seeded in cell culture flasks (approximately 50,000 cells/cm^2). These cells of passage 0 were cultivated under standard culture conditions at 37°C in a humidified 5% CO_2 atmosphere with a change of standard cell culture medium twice a week until their colonies were confluent and the cells were cryopreserved to allow further storage. All utilized cells for the here presented experimental setup were expanded under standard culture conditions to an 80–90% confluence of the cell monolayer in passage 3. The MSC were then synchronized for 24 h using standard cell culture medium supplemented with 1% FBS. After replacement of the low-level FBS concentration, the cells were again cultivated for 24 h in standard cell culture medium before being detached enzymatically by trypsinization to be used in the experiments. A specific characterization of equine adipose tissue-derived MSC has already been published by our group[38,39].

Tendon Scaffold Preparation

Superficial digital flexor tendon specimens of adult warmblood horses were recovered from fresh cadaver limbs obtained at a local abattoir. Dissected tendon samples underwent an overnight incubation at 4°C in PBS (Sigma Aldrich, St. Louis, MO, USA) supplemented with 2% penicillin streptomycin and 0.1% gentamycin, followed by further washing steps using 70% ethanol as well as PBS. Afterwards, tendon specimens were stored at 80°C. Thereafter, a decellularization procedure was applied and included in total five repeated freeze-thaw cycles in liquid nitrogen, a 48-h incubation in hypotonic solution, a 48-h incubation in 1 M Tris buffer (Carl Roth, Karlsruhe, Germany) containing 1% Triton X-100 (Carl Roth, Karlsruhe, Germany) (pH 7.6) as well as several washing steps. The latter ones comprised two consecutive 15-min washing steps in distilled water, a 24-h washing step in standard cell culture medium, and a 24-h washing step in PBS. The decellularization effectiveness of the applied protocol have previously been described by Burk et al. (reduction in resident cells of 99%, residual DNA content of 20%)[40]. Finally, decellularized tendon samples were stored in sterile sampling bags at −80°C. To further customize the size of the tendon scaffolds to 10 mm x 10 mm x 0.3 mm (real-time PCR) and 10 mm x 5 mm x 0.3 mm (histology and LIVE/DEAD® staining), the scaffolds were placed in a cryostat (CM 3050 S; Leica Microscope CMS, Wetzlar, Germany) at a working temperature of −20°C. Initially, full-thickness tendon specimens were cut manually (scalpel blades no. 22) to pieces of 10 mm x 10 mm. Afterwards, these tendon pieces were sliced using the cryostat into tendon scaffolds with a thickness of 0.3 mm[41].

Scaffold Loading with Growth Factors and Scaffold Seeding with Mesenchymal Stromal Cells

The tendon scaffolds were placed into 24-well plates coated with an ultra-low attachment surface (Corning® Costar® Ultra Low attachment multiwell plates; Corning, Corning, NY, USA). This covalently bound hydrogel layered surface was chosen to prevent cellular attachment and protein absorption. Every well was prepared in advance with a small amount of PBS (100 µl PBS applied as one central droplet per well) to allow easy placement of tendon matrices. Subsequently, tendon scaffold surfaces (area of 1 cm^2 each) were coated with either 300 ng TGFβ3 [recombinant human TGFβ3 (CHO-expressed) protein, carrier free; R&D Systems, Minneapolis, MN, USA], 300 ng BMP12 [recombinant human GDF7 (Escherichia coli-derived) protein, carrier free; R&D Systems, Minneapolis, MN, USA], 300 ng TGFβ3 and 300 ng BMP12, or no growth factors (control group). The amount of applied growth factor was related to the initial seeding density of MSC, which were seeded onto the scaffolds 24 h after the growth factor preloading. This means that scaffolds preloaded with 300 ng growth factor were seeded with 0.3 x 10^6 MSC after an incubation of 24 h at 37°C in a 5% CO_2 atmosphere (300 ng growth factor per 0.3 x 10^6 cells). Both applied growth factors were diluted (concentration of 10 µg/ml) in PBS containing 1% BSA (herein referred to as RD) [Reagent Diluent Concentrate 2 (10x); R&D Systems, Minneapolis, MN, USA]. The volume of 30 µl growth factor solution (containing 300 ng growth factor) was pipetted onto the tendon scaffold surface in a meandering loop pattern. Careful drop by drop pipetting ensured the precise placement of the growth factor solution. There was no leakage of pipetted growth factor solution apparent and the scaffold surface was homogeneously preloaded. Coated tendon scaffolds were incubated for 24 h at 37°C in a humidified 5% CO_2 atmosphere and then seeded with synchronised equine MSC of passage 3. This preloading

Table 1. Semi-Quantitative Score System for Macroscopic Evaluation of Scaffold Morphology as well as for Microscopic Evaluation of Cell Distribution Cell Integration.

Score points	Description of cell distribution	Description of cell integration (Given percentages are relative to the total cell number)	Description of scaffold morphology
0	None	None	None
1	Isolated cells	Integration of <10%	1 edge out of 4 is rolled up
2	Focal cell clusters	Integration of 10 – 50%	2 or 3 edges out of 4 are rolled up
3	Continuous and even cell layer	Integration of >50%	All edges are rolled up

technique had been tested in advance by quantifying the amount of TGFβ3 released from the scaffolds with enzyme-linked immunosorbent assay (ELISA) technology (unpublished data). For scaffold seeding, a cell number of 0.3 x 10^6 MSC / 30 µl / cm^2 was distributed evenly on the preloaded scaffold surfaces and allowed to attach for 6 h. Thereafter, 1 ml standard cell culture medium was added and the seeded scaffolds were cultured for 3 and 5 days.

Equine MSC in monolayer culture were treated with the corresponding growth factor containing RD solutions. A number of 0.03 x 10^6 plated cells received 30 ng growth factor, which was supplemented to 3 ml of standard cell culture medium (concentration of 10 ng/ml). Thereby, in accordance with the scaffold culture, the amount of applied growth factor again was related to the initial seeding density of MSC cultured as monolayer (30 ng growth factor per 0.03 x 10^6 cells).

Macroscopic Evaluation of the Scaffold Morphology

To evaluate morphological changes in form of cell-mediated scaffold contraction, all seeded tendon scaffolds were scored macroscopically 3 and 5 days after seeding by two independent observers blinded to the sample group. Table 1 shows the applied rating system for semi-quantitative assessment.

Histology

For an evaluation of the cell distribution and cell integration into the scaffold, MSC-seeded scaffolds with a size of 10 mm x 5 mm x 0.3 mm were fixed in 4% paraformaldehyde (Roti® Histofix 4%; Carl Roth, Karlsruhe, Germany) for 7 days and embedded in paraffin. This was followed by hematoxylin (haematoxylin solution by Gill II; Dr. K. Hollborn & Söhne, Leipzig, Germany) and eosin (eosin 1% aqueous; Dr. K. Hollborn & Söhne Leipzig, Germany) staining of three longitudinal 5 µm sections from the central part of each sample. Two independent observers blinded to the sample group scored the entire paraffin sections microscopically (10x magnification; Leica DMi1, Leica MC 170HD, Leica Microscope CMS, Wetzlar, Germany) according to the semi-quantitative rating system shown in Table 1. While for the evaluation of the cell distribution only superficially adherent MSC were used, the analysis of the cell integration included the proportion of cells that was within deeper scaffold layers. The scoring of the cell distribution aimed to characterize the cell distribution of scaffold-seeded MSC at day 3 and 5 in longitudinal sections. Additionally, the proportion of MSC that immigrated to deeper layers of the tendon scaffold was assessed at day 3 and 5 (cell integration).

To further evaluate cell viability as well as cell body shape and cell alignment of MSC cultured for 3 or 5 days on decellularized tendon, scaffolds with a size of 10 mm x 0.5 mm x 0.3 mm, LIVE/DEAD® staining of MSC-seeded scaffolds was performed using the respective staining kit [LIVE/DEAD® Viability / Cytotoxicity Kit, for mammalian cells; Thermo Fisher Scientific, Karlsruhe, Germany; calcein AM 4 mM in anhydrous DMSO, ethidium homodimer I 2 mM in DMSO / H_2O 1:4 (v/v)] according to the manufacturer's instructions. Three randomly chosen regions of each stained scaffold sample were digitally imaged at 4x magnification (Keyence BZ 9000E, BZ II Analyzer 2.2 Software; Keyence Corporation, Osaka, Japan).

Real-Time PCR

Gene expression was analyzed by real-time PCR and included genes encoding for tendon extracellular matrix molecules (collagen 1A2, collagen 3A1, decorin, tenascin c) and for tendon differentiation markers (scleraxis, smad8, mohawk). Furthermore, the gene expression of collagen 2A1 and osteopontin was assessed to examine potential induction of chondrogenic or osteogenic differentiation. GAPDH and ACTB served as housekeeping genes. Table 2 shows the primer sequences.

Total RNA of monolayer cells was isolated using the RNeasy® Mini Kit with On Column DNase digestion (Qiagen, Hilden Germany) according to instructions of manufacturers. Frozen tendon constructs were homogenized with the Tissue Lyser II (Qiagen). After complete homogenization with proteinase k at 55°C (Qiagen), total RNA was isolated using the RNeasy® Mini Kit with On Column DNase digestion (Qiagen). RNA was quantified with the NanoDrop2000 Spectrophotometer and 1.5 µg of RNA was converted to first-strand cDNA using Reverse Transcriptase RevertAid H Minus (Thermo Fisher Scientific / Life Technologies, Karlsruhe, Germany). cDNA was mixed with primers and iQ™ SYBR Green Supermix (Bio-Rad Laboratories, Hercules, CA, USA). Relative quantification of cDNA was performed and monitored with an Applied Biosystems™ 7500 Real Time PCR System (Applied Biosystems, Foster City, CA, USA). Relative gene expression ratios were calculated using the Pfaffl method and normalized to those of the respective control groups (scaffold and monolayer cultures

Table 2. Primer Sequences for Quantitative Real-Time PCR.

Equine gene	Primer pair sequences	Accession no.	PCR product in bp
ACTB	For: ATCCACGAAACTACCTTCAAC Rev: CGCAATGATCTTGATCTTCATC	NM_001081838.1	174
GAPDH	For: TGGAGAAAGCTGCCAAATACG Rev: GGCCTTTCTCCTTCTCTTGC	NM_001163856.1	309
Col1A2	For: CAACCGGAGATAGAGGACCA Rev: CAGGTCCTTGGAAACCTTGA	XM_001492939.3	243
Col2A1	For: ATTGTAGGACCCAAAGGACC Rev: CAGCAAAGTTTCCACCAAGG	NM_001081764.1	199
Col3A1	For: AGGGGACCTGGTTACTGCTT Rev: TCTCTGGGTTGGGACAGTCT	XM_001917620.3	216
Scleraxis	For: TACCTGGGTTTTCTTCTGGTCACT Rev: TATCAAAGACACAAGATGCCAGC	NM_001105150.1	51
Osteopontin	For: TGAAGACCAGTATCCTGATGC Rev: GCTGACTTGTTTCCTGACTG	XM_001496152.3	158
Decorin	For: ACCCACTGAAGAGCTCAGGA Rev: GCCATTGTCAACAGCAGAGA	NM_001081925.2	239
Tenascin-C	For: TCACATCCAGGTGCTTATTCC Rev: CTAGAGTGTCTCACTATCAGG	XM_001916622.3	163
Mohawk	For: AAGATACTCTTGGCGCTCGG Rev: ACACTAAGCCGCTCAGCATT	XM_014737017.1	170
Smad8	For: AGCCTCCGTGCTCTGCATT Rev: CCCAACTCGGTTGTTTAGTTCAT	AB106117.1	200

without growth factors)[42]. Data are presented as "fold change" increase ($FC_i = (ratio_{treated} / ratio_{control}) - 1$) or decrease ($FC_d = 1 / (ratio_{treated} / ratio_{control}) - 1$).

Image Processing

A combined image processing chain was applied to detect and quantify cells in a consistent manner for both, the LIVE and the DEAD microscopic images (Fig 1). All calculations were performed with Wolfram Mathematica version 11.1 (Wolfram Research, Inc., 2017, Champaign, IL, USA).

In a first step, a difference-of-Gaussian (DoG) filter was applied to enhance cell features and to reduce the global illumination inconsistencies that are typical for fluorescence images (Fig 1B). To further remove background noise a total variation (TV) filter was applied[43]. As shown in Fig 1C, this non-linear filter reduces the noise in the background without smoothing significant cell edges. Note that, for Fig 1C, extreme values of the TV filter were used to make the effect visible. At this stage, a global thresholding was applied to separate the cells from the background which results in a binary image where cells are white and background black.

The binary image was used in a connected component analysis that assigns all pixels belonging to the same cell the same unique number[44]. Therefore, a connected component represents one unique cell in an image. This is indicated by the highlighted cells in Fig 1D. For each component, several morphological measures were computed, i.e. the area, the cell orientation, the bounded disk coverage, and the elongation of the cell.

To obtain only valid cells for the analysis, the area measure was employed to remove image components that are too small. Furthermore, as the processing chain enhances features in very dark regions, the mean pixel value of the component was used to remove invalid elements. All remaining image components were used in further calculations.

To find correct values for the filters that can be used for all images, the first author adjusted the image processing steps for a subset of ten representative images. The mean values of the found parameters were then utilized for all images and are given in Table 3.

Cell Analysis

To obtain a measure for how similar cells are orientated, a circular statistic was used to calculate to which degree the cells in an image deviate from the main growth direction. For this, the orientation of all cells was used to estimate the parameters of a wrapped normal distribution. While the mean orientation is uninteresting as it depends on how scaffolds were prepared, the deviation from the mean orientation is a good indicator for accessing if the cells grow in similar directions (Fig 1E).

To quantify the shape of the cells, an additional measure was computed that favors elongated cells and penalizes round structures. The formula used is the linear combination 3/4*(1 – BCD) + 1/4*Elongation. Here, BCD is the coverage of the bounding disk area by the component area and Elongation is given by 1 (width of the component)/(height of the component). Both measures are indicators for the slenderness of cells.

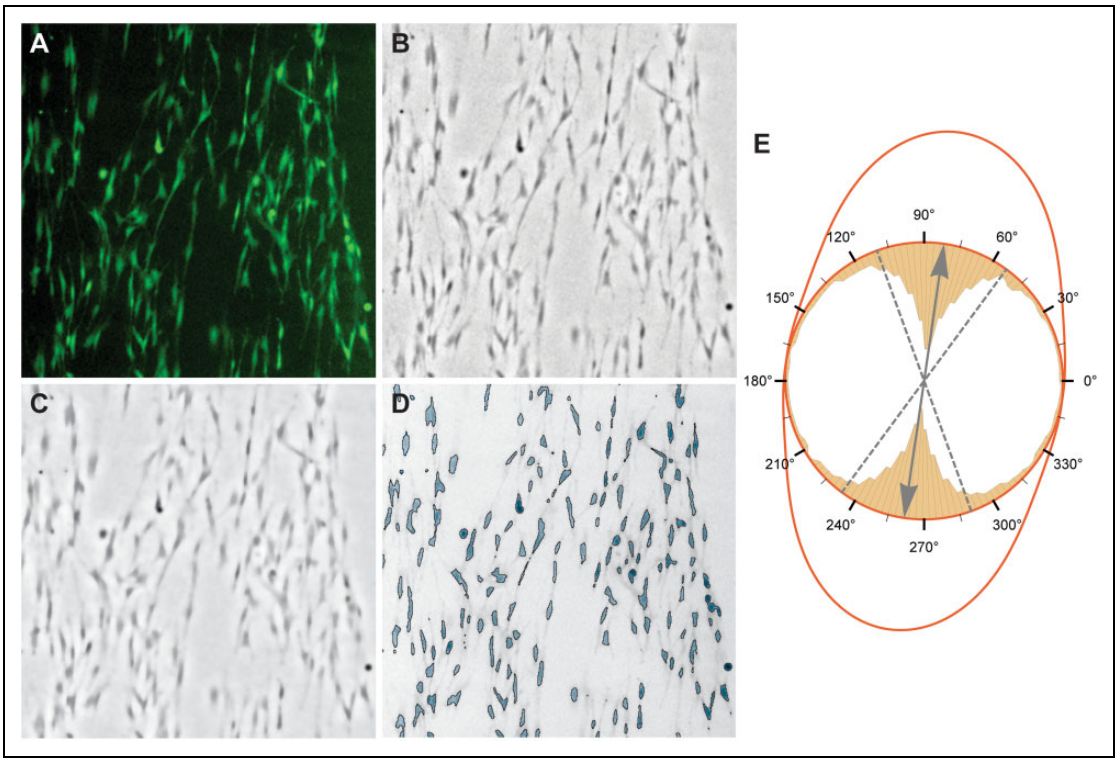

Fig 1. Processing steps for the feature extraction algorithm that was used to quantify cell structures in LIVE images. (A) 512x512 pixel region from an original fluorescence image. (B) Difference-of-Gaussian (DoG)-filtered image of the green channel of (A) to enhance cell details and remove global illumination inconsistencies that usually appear in fluorescence images. (C) Total variation (TV)-filtered version of (B) to reduce background noise and enhance cell edges. (D) Global binarization of (C) followed by an image component analysis to extract cell features. (E) Combined plot of the circular histogram of cell orientations in the example image and the estimated wrapped normal distribution. The inner yellow bar chart represents the distribution of cell orientations with a clear peak at about 80°. Using these cell orientations from an image, the mean and standard deviation (SD) of a wrapped normal distribution can be estimated. The normal distribution is indicated by the red line, while its mean is represented by the grey arrow and SD by the dashed grey lines.

Table 3. Used Image Filter Parameters for Both LIVE and DEAD Cell Processing.

Filter Parameter	Value for Live Cells	Value for Dead Cells
Radius 1 for DoG	2	1
Radius 2 for DoG	24	15
TV Filter	0.0323	0
Binarization Threshold	1.15	1.4
Minimal Component Size	50	15
Minimal Mean Component Brightness	0.1	0.15

Statistical Analysis

Statistical data analysis was performed by using SPSS® Statistics 23.0 software (IBM Deutschland, Dusseldorf, Germany). For the final statistical analysis, median values of sample technical replicates and median values of two independent observers were used. Differences between the experimental groups were analysed with Friedman tests and Wilcoxon signed rank tests. The level of significance was defined at $p = 0.05$.

Results

Scaffold Morphology

Macroscopic evaluation of the scaffold morphology revealed cell-mediated matrix contractions resulting in rolled-up edges in all groups, which further increased between day 3 and day 5 in all groups. However, in the TGFβ3 and TGFβ3/BMP12 groups, scaffold contraction scores were higher compared with the control and BMP12 groups at day 3 ($p < 0.05$) (Fig 2A). The right panel of Fig 3 shows representative images of MSC-mediated changes in the morphology of scaffolds preloaded with and without growth factors as well as a representative image of an unseeded control scaffold.

Cell Distribution and Cell Integration

Hematoxylin and eosin (H&E) staining of longitudinal sections (representative images are depicted in the left panel of Fig 3) showed that there was a consistent cell distribution in all groups at day 3 and day 5 (Fig 2B; Fig 3).

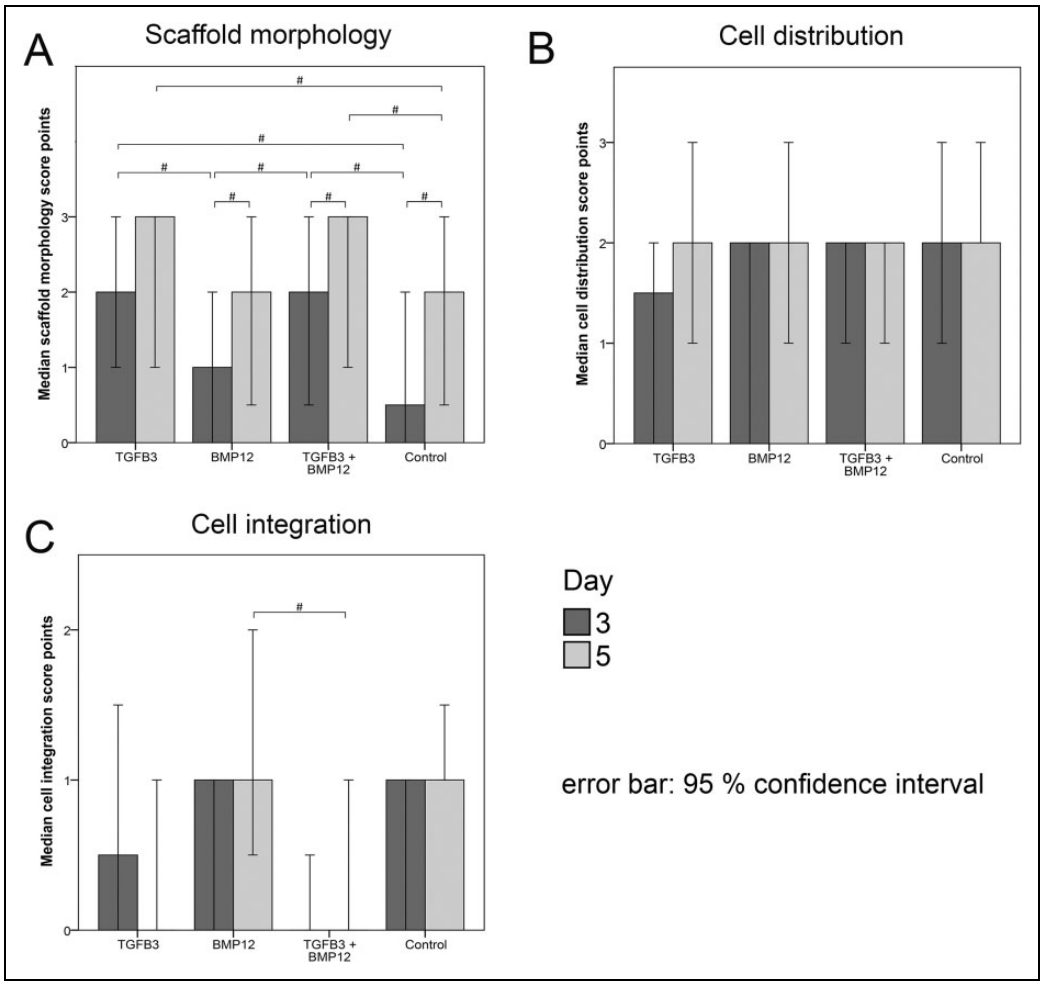

Fig 2. Median score points for morphology (A), cell distribution (B) and cell integration (C) of mesenchymal stromal cells (MSC)-seeded tendon scaffolds. Morphology (A) of MSC-seeded scaffolds preloaded with TGFβ3, BMP12, TGFβ3, and BMP12 or without any growth factor was assessed macroscopically after 3 and 5 days. Hematoxylin and eosin (H&E)-stained paraffin sections of MSC-seeded scaffolds were evaluated for cell distribution (B) and cell integration (C) after 3 and 5 days (10x magnification). Applied rating systems are given in Table 1. Bars represent the median values and error bars the 95% confidence interval; # indicates significant differences between the marked sample groups ($p < 0.05$).

Cell integration was low in all groups with no significant increase between day 3 and day 5. Control scaffolds and BMP12 scaffolds were assigned the highest and TGFβ3/BMP12 scaffolds the lowest score points, resulting in significant differences between these groups at day 5 ($p < 0.05$) (Fig 2C; Fig 3).

Cell Alignment, Shape and Viability

Evaluation of the cell orientation showed that scaffold-seeded cells of all groups tended to be more parallel aligned one to another at day 3 and day 5 than monolayer-cultured cells. However, standard deviations (SD) of cell orientation were not significantly different (Fig 4A).

Analysis of cell body shape indicated a more elongated cell shape for scaffold cultures than for monolayer cultures in all groups at day 3. Scaffolds of the TGFβ3 group were assigned higher score points than scaffolds of the TGFβ3/BMP12 group at day 3 and day 5 ($p < 0.05$). Control scaffolds at day 5 received lower score points than scaffolds of the TGFβ3 and the BMP12 group ($p < 0.05$). Similarly, in monolayer cultures, MSC of the TGFβ3 and the BMP12 group exhibited a more slender appearance than cells of the control group ($p < 0.05$) (Fig 4B).

The numbers of viable cells in scaffold as well as in monolayer cultures at day 3 and day 5 tended to be higher in the BMP12 group and the control group than in the TGFβ3 and TGFβ3/BMP12 groups. The monolayer TGFβ3/BMP12 group contained significantly fewer numbers of viable cells than the monolayer BMP12 and control groups ($p < 0.05$) at both time points. At day 5, additionally, the monolayer cultures supplemented with TGFβ3 had lower viable cell counts than the BMP12 and control monolayer groups ($p < 0.05$) (Fig 4C).

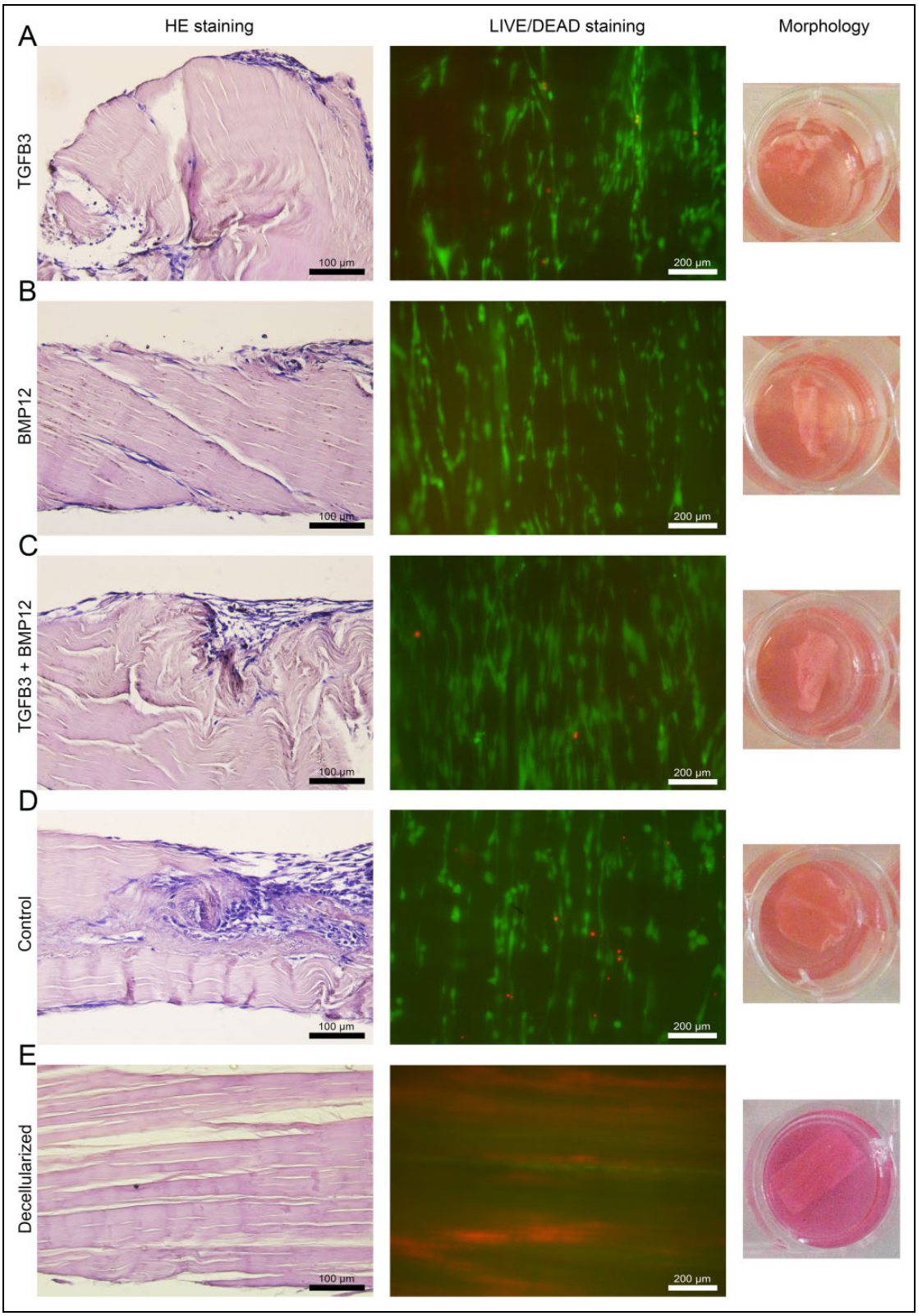

Fig 3. Microscopic and macroscopic appearance of MSC-seeded tendon scaffolds and an unseeded control. Representative images of H&E-stained paraffin sections (left) of MSC-seeded scaffolds preloaded with TGFβ3 (A), BMP12 (B), TGFβ3, and BMP12 (C) or without any growth factor (D) (20x magnification; calibration marks correspond to 100 µm). Corresponding images of the LIVE/DEAD® staining (middle) and the macroscopic appearance of the scaffolds (right) are given. In fluorescence microscopic images of the LIVE/DEAD® staining presented in the middle panel, vital cells are indicated by green fluorescence (display of intracellular esterase activity), cells with defect cellular membranes show a red fluorescence signal of their nucleus (10x magnification; calibration marks correspond to 200 µm). Adequate images of unseeded control scaffold are added at the bottom to reflect the most likely cellular origin of morphological changes in MSC seeded scaffolds. All images were taken on day 5 from samples, which received MSC of one single donor.

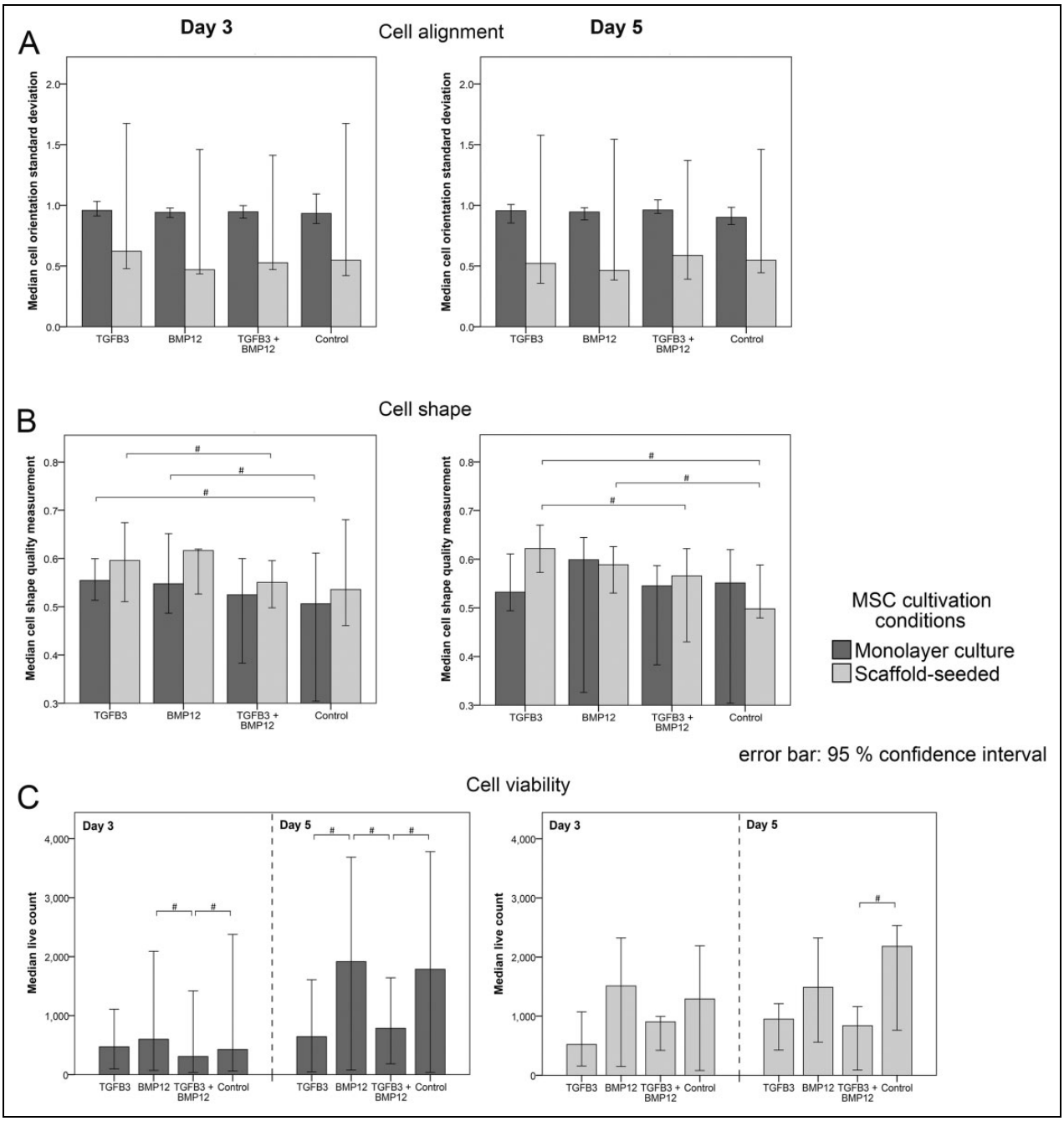

Fig 4. Results of the quantitative analysis of images of LIVE/DEAD®-stained MSC-seeded tendon scaffolds and MSC monolayer cultures. Median values of the cell orientation standard deviation (A), the cell shape quality measurement (B) and of the counted live cells (C) assessed in monolayer-cultured and scaffold-seeded cells supplemented with TGFβ3, BMP12, TGFβ3, and BMP12 or without any growth factor at day 3 and day 5. High values of the cell orientation standard deviation mean that the majority of cells is not aligned parallel to a defined main direction and thereby indicating a less marked parallelism one to another. The scale for the cell shape quality measurement includes values between zero (round cell body shape) and one (elongated cell body shape). Bars represent median values and the error bars the 95% confidence interval; # illustrates significant differences between the marked sample groups ($p < 0.05$).

Representative fluorescence microscopic images of the LIVE/DEAD® staining of MSC-seeded tendon scaffolds preloaded with and without growth factors as well as a representative image of an unseeded control scaffold are presented in the middle panel of Fig 3.

Scaffold-induced Changes in Gene Expression

Without the addition of growth factors (control groups; data not shown), scaffold culture increased decorin (10-fold increase at day 3 and 4-fold increase at day 5) and

osteopontin expression (43-fold increase at day 3 and 39-fold increase at day 5) compared with monolayer culture. There was also a scaffold-induced upregulation of the tenascin c expression observed at day 5 (2-fold) but not at day 3. However, scaffold culture decreased smad8 expression (2-fold decrease at day 3 and 3-fold decrease at day 5). At day 5, additionally, collagen 1A2 (3-fold decrease) and scleraxis expression (9-fold decrease) were decreased compared with the monolayer culture. While these differences were significant ($p < 0.05$), no further changes in gene expression were observed due to scaffold culture alone.

Growth Factor-Induced Changes in Gene Expression

Extracellular matrix molecules. Collagen 1A2 upregulation was induced by TGFβ3 and TGFβ3/BMP12 in monolayer cultures, but further downregulation was induced by TGFβ3/BMP12 in scaffold cultures, which was more markedly observed at day 3. BMP12 alone had no effect on collagen 1A2 expression, resulting in gene expression ratios similar to the respective controls. Consequently, similar as observed in the controls without growth factors, collagen 1A2 gene expression ratios were lower in all growth factor scaffold groups compared with the correspondingly treated monolayers at day 5. Furthermore, although the fold changes of up- and downregulation of collagen 1A2 compared with the controls were not high, differences between gene expression ratios of TGFβ3 and TGFβ3/BMP12 groups compared with the respective BMP12 and control groups were found to be significant at days 3 and 5 (Fig 5A).

Collagen 3A1 expression following growth factor treatment showed very similar trends and differences as collagen 1A2 expression. However, the fold changes compared with the controls were higher and the impact of TGF3 and TGFβ3/BMP12, upregulating collagen 3A1 expression in monolayer cultures and downregulating collagen 3A1 expression in scaffold cultures, was overall more pronounced at day 5 (Fig 5B).

Decorin expression in monolayer cultures was slightly upregulated in all groups (including the control group) at both time points and therefore depicted fold changes have small numbers. In scaffold cultures, TGFβ3 and TGFβ3/BMP12 induced a strong downregulation of decorin compared with the control and BMP12 scaffold cultures, which was significant at day 3 and day 5 (Fig 5C). This reversed the scaffold-induced upregulation of decorin and resulted in similar gene expression ratios of scaffold and monolayer TGFβ3 and TGFβ3/BMP12 groups at day 5 (data not shown).

Tenascin c was strongly upregulated by TGFβ3 and TGFβ3/BMP12 in both monolayer and scaffold cultures compared with the control as well as BMP12 groups at day 3. This upregulation was maintained in the monolayer cultures until day 5, but, despite the upregulation induced by the scaffold alone, this was not the case in the scaffold cultures, leading to significant differences between these approaches (Fig 5D).

Osteopontin expression was strongly upregulated by TGFβ3 and TGFβ3/BMP12 in the monolayer groups at day 3 and increased further until day 5. However, in the scaffold groups, it was downregulated by BMP12 and TGFβ3/BMP12, which was significant for BMP12 at day 3 and TGFβ3/BMP12 at day 5 (Fig 5E). Similar as observed for decorin, the growth factor-mediated downregulation in scaffold cultures reversed an obtained scaffold-induced upregulation of osteopontin (data not shown).

Collagen 2A1 was not expressed at detectable levels in any group. Fold change gene expression relative to the respective controls incubated without growth factors and significance of differences between gene expression ratios is detailed in Fig 5A–E.

Intracellular tendon markers. Scleraxis upregulation was induced by TGFβ3 and TGFβ3/BMP12 in monolayer cultures, which was evident at day 3 and day 5, while BMP12 alone again had no consistent effect on scleraxis expression. In scaffold cultures, no major effect on scleraxis expression could be observed with any of the growth factors tested (Fig 6A). Consequently, similar as observed in the controls without growth factors, scleraxis gene expression ratios were significantly higher in all monolayer groups compared with the correspondingly treated scaffold groups at day 5 (data not shown).

Smad8 appeared to be downregulated in scaffold cultures with TGFβ3 and TGFβ3/BMP12 at day 3. Although this was found to be significant compared with the respective control and BMP12 scaffold groups, growth factor-induced differences in smad8 expression were overall minor (Fig 6B). However, due to the scaffold-induced downregulation, smad8 gene expression ratios were significantly lower in all scaffold groups compared with the correspondingly treated monolayers at day 3 and day 5 (data not shown).

Mohawk expression was inconsistent and largely similar to the respective controls in all groups except the monolayer TGFβ3 group which showed a consistent but still weak upregulation of mohawk (Fig 6C).

Fold change gene expression relative to the respective controls incubated without growth factors and significance of differences between gene expression ratios is detailed in Fig 6A–C.

Discussion

The present study aimed to investigate the potential synergistic effects of TGFβ3 and BMP12 in the microenvironment of tendon ECM. With high relevance for regenerative tendon therapies and tendon tissue engineering, we could show that growth factor-driven tenogenic induction is altered by topographical and biochemical cues from decellularized tendon scaffolds, thus depends strongly on the microenvironment.

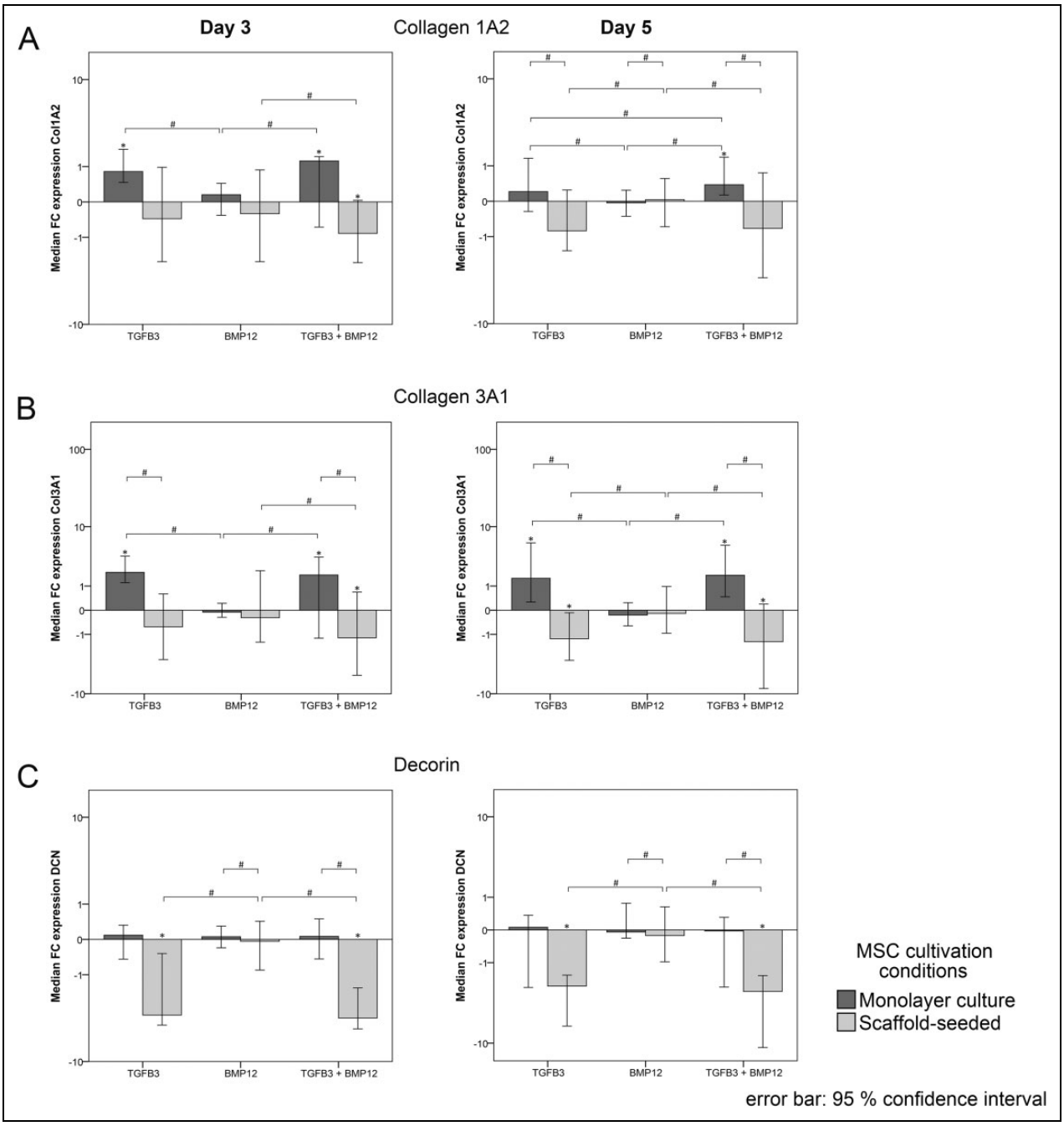

Fig 5. Gene expression levels of extracellular matrix components. Gene expression of monolayer and scaffold cultures was analysed at day 3 (left) and at day 5. Data are presented as median "fold change" (FC) to the respective control of the monolayer and the scaffold culture, which received no growth factor supplementation and is displayed as horizontal line intersecting the *x*-axis at zero. Bars represent the median values and error bars the 95% confidence interval; * indicates significant differences compared with the respective control ($p < 0.05$); # illustrates significant differences between the marked sample groups ($p < 0.05$).

In the evaluated experimental setup, TGFβ3 and BMP12 were preloaded onto decellularized tendon ECM matrices to create a functionalized scaffold providing bioactive growth factors in a localized form. At the same time, these matrices aim to closely reflect the architecture and ECM composition of native tendons, potentially providing natural cues for cell differentiation. This methodological approach allowed interactions of the growth factors with both the tendon ECM components as well as the seeded MSC in a rather narrow niche. Furthermore, early conformational changes due to interactions between applied growth factors and ingredients of surrounding standard cell culture medium could be

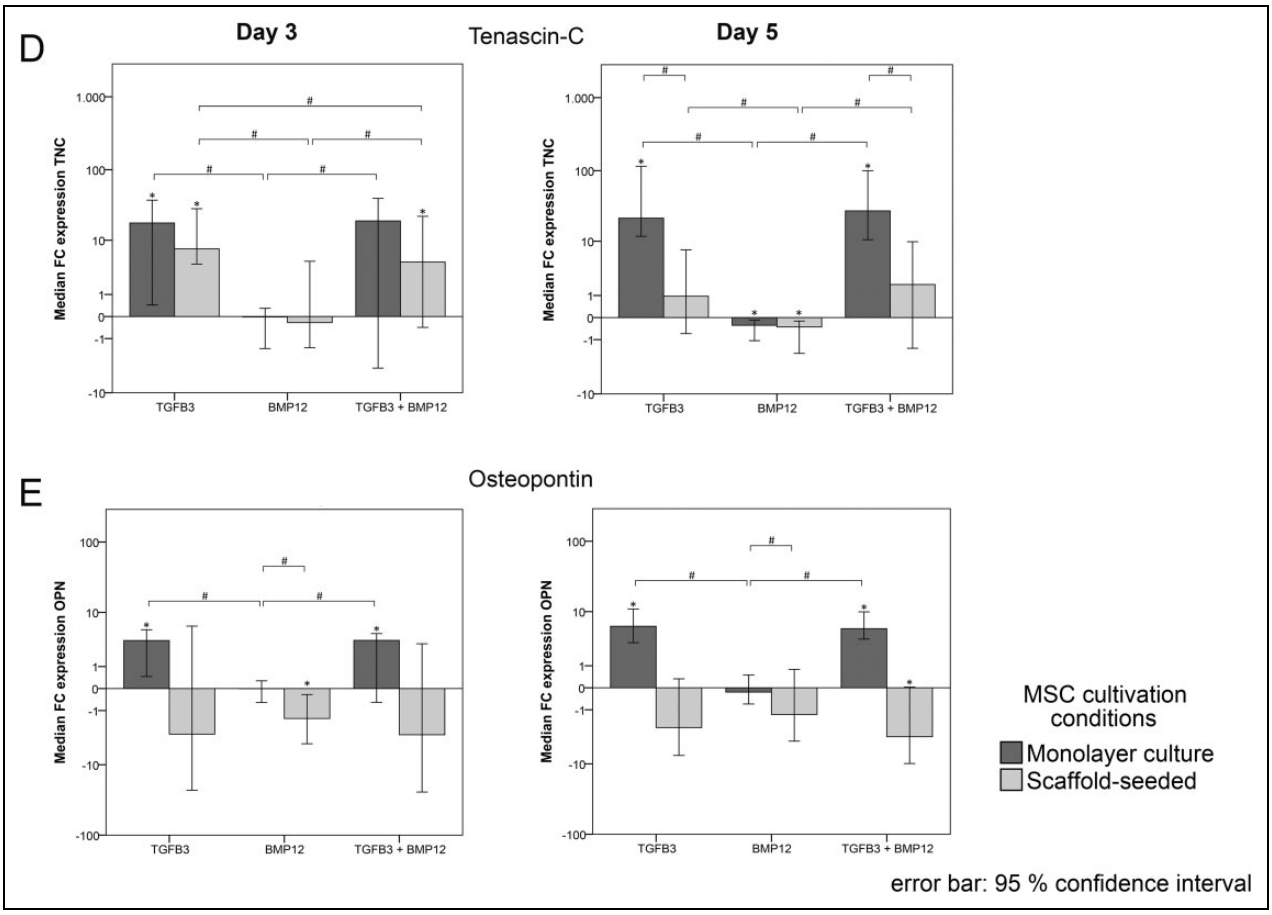

Fig 5. (Continued).

avoided. A scaffold binding rate of roughly 70% was demonstrated by ELISA technique prior to this study (unpublished data). However, limiting effects on growth factor activity could be due to possible conformational changes, which are strongly sensitive to local microenvironment (oxygen tension, pH value, temperature). Other studies successfully applied TGFβ3 controlled-release chitosan scaffolds or TGFβ3-loaded RGD-coupled alginate microspheres to induce tenogenic differentiation of seeded cells *in vitro* as well as *in vivo*[45,46]. However, to the best of our knowledge, there have been no studies including tendon matrix-coupled TGFβ3 and BMP12 to induce tenogenesis of equine MSC *in vitro*.

Cell-mediated contractions of seeded scaffolds were observed. Interestingly, this effect was not described in a study that cultured equine tendon- as well as bone marrow-derived cells on acellular tendon matrices of the same size used in this work[47]. Although in this study, supplementation with insulin-like growth factor-I (IGF-I) increased cell numbers and collagen synthesis of tendon-derived and matrix-seeded cells, there were no cell-mediated matrix contractions in the presence of IGF-I. However, our results showed that scaffold contractions were significantly promoted by TGFβ3. Further research is needed to investigate the molecular mechanisms of TGFβ3-driven scaffold contractions.

Generally, MSC use clustered complexes of integrins, so-called focal adhesions, to exert traction forces generated by intracellular contractile elements on the surrounding matrix. This process is called mechanotransduction and enables cells to gauge the resistance of the surrounding ECM to the cellular traction forces[48–50]. Moreover, recent research indicates cellular traction forces to rearrange ECM adhesion ligands and to change effects resulting from ECM-integrin binding[51]. Referring to ECM-bound TGFβ, cellular traction forces are able to cause structural changes in integrin-bound TGFβ so that TGFβ molecules were unveiled and can bind to surface receptors of the same or neighbouring cells[52].

The morphological evaluation of MSC revealed a more pronounced scaffold induced parallel orientation of MSC in scaffold cultures when compared with monolayer cultures (Fig 4A). This tendon matrix-induced tenocyte-like orientation was already described in equine MSC cultured on decellularized tendon matrices, and the current study indicated that this effect is TGFβ3- and BMP12-independent[10].

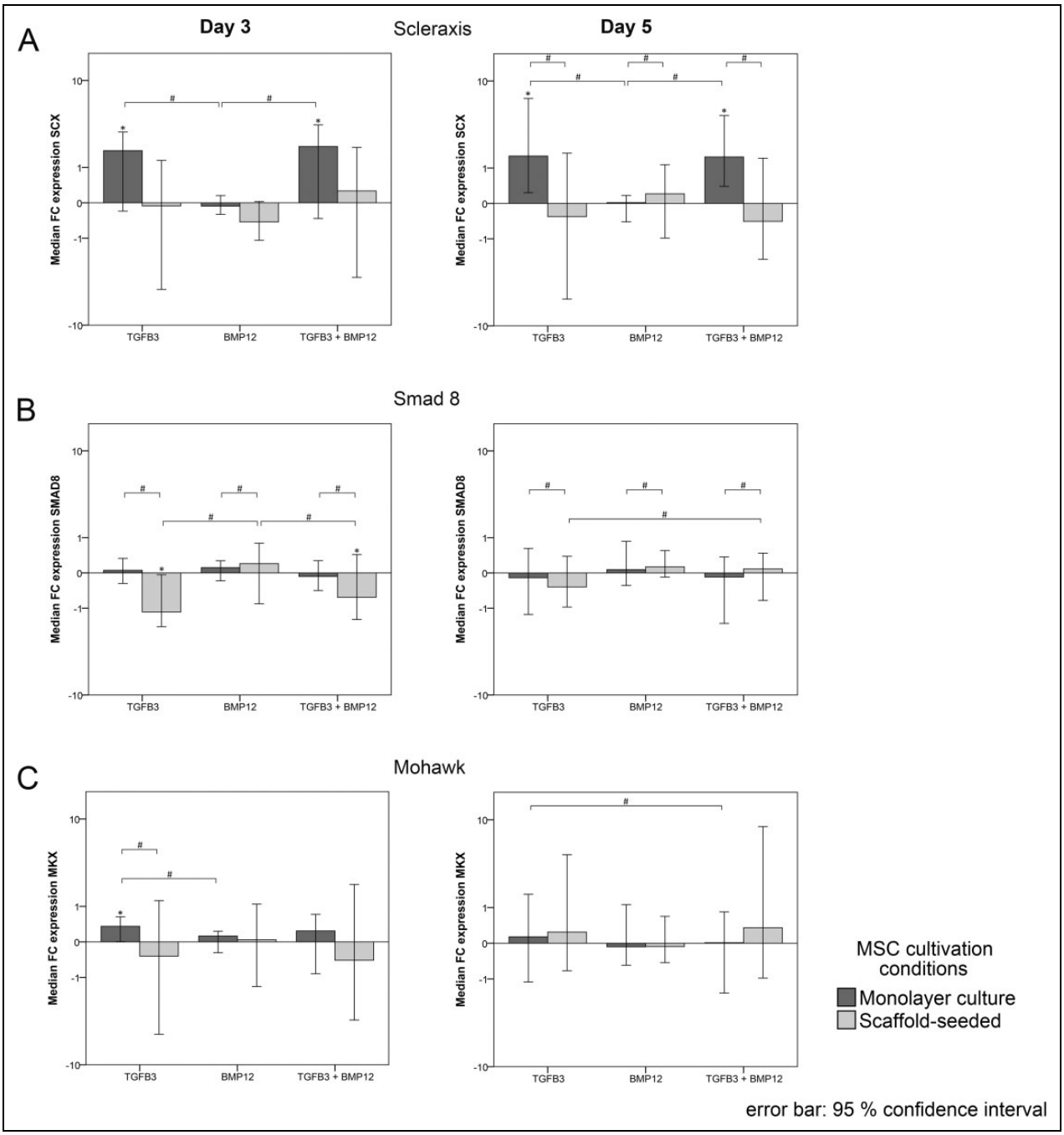

Fig 6. Gene expression level of intracellular tendon markers. Gene expression in monolayer cultured and scaffold-seeded cells was assessed at day 3 (left) and at day 5 (right). Data are presented as median FC to the respective control of the monolayer and the scaffold culture, which received no growth factor supplementation and is displayed as horizontal line intersecting the *x*-axis at zero. Bars represent the median values and error bars the 95% confidence interval; * indicates significant differences compared with the respective control ($p < 0.05$); # illustrates significant differences between the marked sample groups ($p < 0.05$).

Nevertheless, the supplementation with either TGFβ3 or BMP12 induced a trend towards slenderer, more elongated cell shapes found in both scaffold and monolayer cultures (Fig 4B). Furthermore, at day 3, the tenocyte-like appearance of elongated MSC was more pronounced in all scaffold groups than in monolayer cultures. This is in accordance with results from a 3-day-culture of equine MSC seeded onto tendon matrices[10]. However, results obtained from the cell shape analysis are rather inhomogeneous and do not indicate a relation to growth factor supplementation, MSC culture conditions as well as to the time point. This could be due to inconsistencies in the automated image segmentation of

the MSC. Additionally, the calculated cell shape parameters might only be weak classifiers for tenogenesis.

The number of viable cells in scaffold as well as in monolayer cultures was smaller in groups supplemented with TGFβ3 alone or combined with BMP12 than in the remaining groups. Although all three mammalian TGFβ isoforms have already been reported to decrease the proliferation of cells from rabbit digital flexor sheaths, epitenon, and tendon, the molecular mechanisms of this growth factor-driven effect is rather unknown[53]. It is presumed that the inhibition of cell growth may be regulated via the TGFβ-driven downregulation of decorin[54]. Recently, TGFβ3 (1 ng/ml) was shown to arrest proliferation of rabbit bone marrow-derived MSC in 2D-culture, while enhancing cellular metabolic activity[55]. Thus, future studies should include complementary assays to quantify DNA and to assess the metabolic activity of scaffold-seeded cells.

A typical gene expression profile of *in vitro* tenogenic differentiation was observed after tenogenic induction using TGFβ3 alone or combined with BMP12 in monolayer cultures. This included increased expression levels of collagen 1A2, collagen 3A1, tenascin c, scleraxis and mohawk, but also osteopontin. The tendon ECM scaffold alone also altered gene expression but not in a tendon-specific manner, most markedly including upregulation of decorin and osteopontin as well as downregulation of smad8. Correspondingly, the combination of growth factors and tendon ECM did not merely increase the TGFβ3-induced effects observed in monolayer culture. Part of these combined effects on gene expression, along with the more tendon-like morphology and cell alignment, suggest a higher specificity of tenogenic induction. However, study limitations included the lack of an earlier time point of analysis (day 1 or earlier) to allow a better understanding of the mechanisms that induce tenogenic induction. Future studies should also include the evaluation of MSC-driven matrix turnover to give further information about the reciprocal character of the MSC-scaffold-interaction (e.g., matrix metalloproteinase 1/13, fragments of collagen 1A2 and fibromodulin).

Collagen 3A1 expression, being upregulated by TGFβ3 in monolayer groups, was downregulated when combining TGFβ3 and scaffold culture. This represents a closer approximation to mature tenocytes as collagen 3A1 is mainly related to immature or repair tendon tissue[56,57]. Furthermore, decorin being upregulated in scaffold groups without TGFβ3, was downregulated when combining TGFβ3 and scaffold culture, again demonstrating an increased specificity of tenogenic differentiation. Decorin, which is the most abundant proteoglycan in tendon tissue, is expressed in MSC cultured as monolayer and even more in MSC seeded onto tendon scaffolds. While short-term cyclic stretching have shown no influence on the decorin expression in tendon scaffold-seeded MSC, the present work demonstrated TGFβ3 as potential regulator of the decorin expression in scaffold-seeded MSC[10,58]. Current research regarding the functional influence of decorin on tendon regeneration have suggested that the reduction of the decorin expression to a certain level enhances tendon maturation as well as the functional restoration of injured tendon tissue[54,59]. Therefore, TGFβ3-treatment of scaffold-seeded MSC may enable an appropriately well-balanced cellular decorin expression. Osteopontin, which was also upregulated by scaffold culture, was downregulated on scaffolds loaded with BMP12 or TGFβ3/BMP12, suggesting that BMP12 may prevent erroneous osteogenic differentiation.

Besides these more tenocyte-specific effects observed, combining TGFβ3 and scaffold culture in the current study, collagen 1A2 gene expression was downregulated, most likely as a response to the protein being abundant in the tendon scaffold in the form of a negative feedback mechanism. The same had been observed in an own previous study involving tendon ECM scaffolds and longitudinal stretching as tenogenic stimuli[10], while others demonstrated collagen 1A2 upregulation using virtually the same approach[60]. This discrepancy could be due to the longer incubation time of 10 days in the latter study or to the different tendon decellularization protocol used for scaffold production, involving sodium dodecyl sulfate[61], potentially leading to ECM alterations[62]. Furthermore, in the current study, scleraxis, which is considered as a more specific tendon differentiation marker[63,64], was downregulated in response to scaffold culture until day 5, despite the presence of TGFβ3. One possible explanation might be that scleraxis upregulation in scaffold culture took place earlier and was only transient, and therefore not detectable at the assessment time points chosen in the current study. However, it is more likely that further factors such as mechanical stimulation are required to maintain scleraxis upregulation in scaffold culture[10,65]. The downregulation of the transcription factor scleraxis in the current study also represents a further aspect potentially contributing to the lower collagen 1A2 expression in scaffold groups.

Results from the present study indicate that BMP12 did not increase the expression of tendon-related markers, either in monolayer cultures or in the presence of decellularized tendon tissue, but rather modulated osteopontin expression. In the current literature, a large methodological variability was found regarding the experimental setup and the applied amounts of BMP12 (1–1000 ng/ml). Possibly, the hypothesized tenogenic induction via BMP12 failed due to an insufficient growth factor availability in the present study design[32,34,66]. Furthermore, promising results from *in vivo* applications of BMP12 delivery systems indicate the high context sensitivity of BMP12[67,68]. Accordingly, potential cues from the scaffold may modulate BMP12 effects. Interestingly, the scaffold-induced downregulation of smad8 observed in the current study might represent a puzzle piece of scaffold-mediated fine-control over cellular differentiation. The receptor regulated smad8, the activation of which was reported to induce tenogenic differentiation, is part of the BMP signal transduction pathways[69]. Therefore, downregulation of smad8 could reduce the effects of BMP12 and

modulate the specificity of downstream transcriptional events in response to the surrounding microenvironment.

The results obtained in this study demonstrate the complex interaction of different tenogenic factors including the growth factors TGFβ3 and BMP12 as well as tendon ECM. TGFβ3 alone induced widely tenocyte-specific properties in MSC in the artificial environment of monolayer culture. However, synergistic but also antagonistic effects were observed when the growth factors were applied in tendon ECM scaffold culture. This observation contributes to the understanding of tenogenic differentiation in the context of tendon tissue engineering but also entails implications for the use of growth factors in tendon cell therapy.

Availability of Data and Material

The datasets supporting the conclusion of this article are available from the corresponding author on request.

Ethical Approval

Ethical approval is not applicable. (All of the donor animals were sacrificed for reasons unrelated to the current study. Therefore, in accordance with national guidelines and the local ethics committee (Landesdirektion 455 Leipzig), no license was required for sample collection).

Statement of Human and Animal Rights

Statement of human and animal rights is not applicable.

Statement of Informed Consent

There are no human subjects in this article and informed consent is not applicable.

Declaration of Conflicting Interests

The author(s) declared no potential conflicts of interest with respect to the research, authorship, and/or publication of this article.

Funding

The author(s) disclosed receipt of the following financial support for the research and/or authorship of this article: The work presented in this paper was made possible by funding from the German Federal Ministry of Education and Research (BMBF 1315883) and the German National Research Foundation (DFG BU3110/1-1). Further co funding was provided by Saxon public tax funds.

Supplemental Material

Supplemental material for this article is available online.

References

1. Yang G, Rothrauff BB, Tuan RS. Tendon and ligament regeneration and repair: Clinical relevance and developmental paradigm. Birth Defects Res C Embryo Today. 2013;99(3): 203–222. doi:10.1002/bdrc.21041.
2. Verdiyeva G, Koshy K, Glibbery N, Mann H, Seifalian AM. Tendon reconstruction with tissue engineering approach–a review. J Biomed Nanotechnol. 2015;11(9):1495–1523. eng.
3. Hess GW. Achilles tendon rupture: a review of etiology, population, anatomy, risk factors, and injury prevention. Foot Ankle Spec. 2010;3(1):29–32. eng. doi:10.1177/1938640009355191.
4. Clayton RAE, Court-Brown CM. The epidemiology of musculoskeletal tendinous and ligamentous injuries. Injury. 2008; 39(12):1338–1344. eng. doi:10.1016/j.injury.2008.06.021.
5. Thomopoulos S, Parks WC, Rifkin DB, Derwin KA. Mechanisms of tendon injury and repair. J Orthop Res. 2015;33(6): 832–839. eng. doi:10.1002/jor.22806.
6. Smith RK, Korda M, Blunn GW, Goodship AE. Isolation and implantation of autologous equine mesenchymal stem cells from bone marrow into the superficial digital flexor tendon as a potential novel treatment. Equine Vet J. 2003;35(1):99–102. eng.
7. Nixon AJ, Dahlgren LA, Haupt JL, Yeager AE, Ward DL. Effect of adipose-derived nucleated cell fractions on tendon repair in horses with collagenase-induced tendinitis. Am J Vet Res. 2008;69(7):928–937. doi:10.2460/ajvr.69.7.928.
8. Godwin EE, Young NJ, Dudhia J, Beamish IC, Smith RKW. Implantation of bone marrow-derived mesenchymal stem cells demonstrates improved outcome in horses with overstrain injury of the superficial digital flexor tendon. Equine Vet J. 2012;44(1):25–32. doi:10.1111/j.2042-3306.2011.00363.x.
9. Smith RKW, Werling NJ, Dakin SG, Alam R, Goodship AE, Dudhia J, Laird EG. Beneficial effects of autologous bone marrow-derived mesenchymal stem cells in naturally occurring tendinopathy. Plos One. 2013;8(9):e75697. doi:10.1371/journal.pone.0075697.
10. Burk J, Plenge A, Brehm W, Heller S, Pfeiffer B, Kasper C. Induction of tenogenic differentiation mediated by extracellular tendon matrix and short-term cyclic stretching. Stem Cells Int. 2016;2016:7342379. eng. doi:10.1155/2016/7342379.
11. Burk J, Berner D, Brehm W, Hillmann A, Horstmeier C, Josten C, Paebst F, Rossi G, Schubert S, Ahrberg AB. Long-term cell tracking following local injection of mesenchymal stromal cells in the equine model of induced tendon disease. Cell Transplant. 2016;25(12):2199–2211. eng. doi:10.3727/096368916X692104.
12. Zhang G, Ezura Y, Chervoneva I, Robinson PS, Beason DP, Carine ET, Soslowsky LJ, Iozzo RV, Birk DE. Decorin regulates assembly of collagen fibrils and acquisition of biomechanical properties during tendon development. J Cell Biochem. 2006;98(6):1436–1449. eng. doi:10.1002/jcb.20776.
13. Yoon JH, Halper J. Tendon proteoglycans: biochemistry and function. J Musculoskelet Neuronal Interact. 2005;5(1):22–34. eng.
14. Zhang J, Li B, Wang JHC. The role of engineered tendon matrix in the stemness of tendon stem cells in vitro and the promotion of tendon-like tissue formation in vivo. Biomaterials. 2011;32(29): 6972–6981. eng. doi:10.1016/j.biomaterials.2011.05.088.
15. Agmon G, Christman KL. Controlling stem cell behavior with decellularized extracellular matrix scaffolds. Curr Opin Solid State Mater Sci. 2016;20(4):193–201. eng. doi:10.1016/j.cossms.2016.02.001.
16. Watt FM, Huck WTS. Role of the extracellular matrix in regulating stem cell fate. Nat Rev Mol Cell Biol. 2013;14(8): 467–473. eng. doi:10.1038/nrm3620.
17. Lui PPY, Rui YF, Ni M, Chan KM. Tenogenic differentiation of stem cells for tendon repair - what is the current evidence? J Tissue Eng Regen Med. 2011;5(8):e144–e163. doi:10.1002/term.424.

18. Kishore V, Bullock W, Sun X, van Dyke WS, Akkus O. Tenogenic differentiation of human MSCs induced by the topography of electrochemically aligned collagen threads. Biomaterials. 2012;33(7):2137–2144. eng. doi:10.1016/j.biomaterials.2011.11.066.
19. Younesi M, Islam A, Kishore V, Anderson JM, Akkus O. tenogenic induction of human mscs by anisotropically aligned collagen biotextiles. Adv Funct Mater. 2014;24(36):5762–5770. eng. doi:10.1002/adfm.201400828.
20. Yang G, Rothrauff BB, Lin H, Gottardi R, Alexander PG, Tuan RS. Enhancement of tenogenic differentiation of human adipose stem cells by tendon-derived extracellular matrix. Biomaterials. 2013;34(37):9295–9306. eng. doi:10.1016/j.biomaterials.2013.08.054.
21. Ning LJ, Zhang YJ, Zhang Y, Qing Q, Jiang YL, Yang JL, Luo JC, Qin TW. The utilization of decellularized tendon slices to provide an inductive microenvironment for the proliferation and tenogenic differentiation of stem cells. Biomaterials. 2015;52:539–550. eng. doi:10.1016/j.biomaterials.2015.02.061.
22. Chang H, Brown CW, Matzuk MM. Genetic analysis of the mammalian transforming growth factor-beta superfamily. Endocr Rev. 2002;23(6):787–823. eng. doi:10.1210/er.2002-0003.
23. Kuo CK, Petersen BC, Tuan RS. Spatiotemporal protein distribution of TGF-betas, their receptors, and extracellular matrix molecules during embryonic tendon development. Dev Dyn. 2008;237(5):1477–1489. eng. doi:10.1002/dvdy.21547.
24. Chan KM, Fu SC, Wong YP, Hui WC, Cheuk YC, Wong MWN. Expression of transforming growth factor beta isoforms and their roles in tendon healing. Wound Repair Regen. 2008;16(3):399–407. eng. doi:10.1111/j.1524-475X.2008.00379.x.
25. Barsby T, Guest D. Transforming growth factor beta3 promotes tendon differentiation of equine embryo-derived stem cells. Tissue Eng Part A. 2013;19(19-20):2156–2165. eng. doi:10.1089/ten.TEA.2012.0372.
26. Kapacee Z, Yeung CYC, Lu Y, Crabtree D, Holmes DF, Kadler KE. Synthesis of embryonic tendon-like tissue by human marrow stromal/mesenchymal stem cells requires a three-dimensional environment and transforming growth factor β3. Matrix Biol. 2010;29(8):668–677. eng. doi:10.1016/j.matbio.2010.08.005.
27. Urist MR. Bone: Formation by autoinduction. Science. 1965;150(3698):893–899. eng.
28. Urist MR, Strates BS. Bone morphogenetic protein. J Dent Res. 1971;50(6):1392–1406. eng.
29. Wolfman NM, Celeste AJ, Cox K, Hattersley G, Nelson R, Yamaji N, DiBlasio-Smith E, Nove J, Song JJ, Wozney JM, Rosen V. Preliminary characterization of the biological activities of rhBMP-12. J Bone Mineral Res. 1995;Suppl.1(10):148.
30. Wang QW, Chen ZL, Piao YJ. Mesenchymal stem cells differentiate into tenocytes by bone morphogenetic protein (BMP) 12 gene transfer. J Biosci Bioeng. 2005;100(4):418–422. doi:10.1263/jbb.100.418.
31. Fu W, Chen G, Tang X, Li Q, Ll J. Effect of recombinant adenovirus-bone morphogenetic protein 12 transfection on differentiation of peripheral blood mesenchymal stem cells into tendon/ligament cells. Zhongguo Xiu Fu Chong Jian Wai Ke Za Zhi. 2015;29(4):472–476. chi.
32. Shen H, Gelberman RH, Silva MJ, Sakiyama-Elbert SE, Thomopoulos S. BMP12 induces tenogenic differentiation of adipose-derived stromal cells. Plos One. 2013;8(10):e77613. eng.
33. Mohanty N, Gulati BR, Kumar R, Gera S, Kumar P, Somasundaram RK, Kumar S. Immunophenotypic characterization and tenogenic differentiation of mesenchymal stromal cells isolated from equine umbilical cord blood. In Vitro Cell Dev Biol Anim. 2014;50(6):538–548. eng. doi:10.1007/s11626-013-9729-7.
34. Lee JY, Zhou Z, Taub PJ, Ramcharan M, Li Y, Akinbiyi T, Maharam ER, Leong DJ, Laudier DM, Ruike T, Torina PJ, Zaidi M, Majeska RJ, Schaffler MB, Flatow EL, Sun HB. BMP-12 treatment of adult mesenchymal stem cells in vitro augments tendon-like tissue formation and defect repair in vivo. Plos One. 2011;6(3):e17531. eng. doi:10.1371/journal.pone.0017531.
35. Forslund C, Rueger D, Aspenberg P. A comparative dose–response study of cartilage-derived morphogenetic protein (CDMP)-1, -2 and -3 for tendon healing in rats. J Orthop Res. 2003;21(4):617–621. doi:10.1016/S0736-0266(03)00010-X.
36. Herpin A, Cunningham C. Cross-talk between the bone morphogenetic protein pathway and other major signaling pathways results in tightly regulated cell-specific outcomes. FEBS J. 2007;274(12):2977–2985. eng. doi:10.1111/j.1742-4658.2007.05840.x.
37. Yang G, Rothrauff BB, Lin H, Yu S, Tuan RS. Tendon-derived extracellular matrix enhances transforming growth factor-beta3-induced tenogenic differentiation of human adipose-derived stem cells. Tissue Eng Part A. 2017;23(3-4):166–176. eng. doi:10.1089/ten.TEA.2015.0498.
38. Burk J, Ribitsch I, Gittel C, Juelke H, Kasper C, Staszyk C, Brehm W. Growth and differentiation characteristics of equine mesenchymal stromal cells derived from different sources. Vet J. 2013;195(1):98–106. doi:10.1016/j.tvjl.2012.06.004.
39. Paebst F, Piehler D, Brehm W, Heller S, Schroeck C, Tarnok A, Burk J. Comparative immunophenotyping of equine multipotent mesenchymal stromal cells: an approach toward a standardized definition. Cytometry A. 2014;85(8):678–687. eng. doi:10.1002/cyto.a.22491.
40. Burk J, Erbe I, Berner D, Kacza J, Kasper C, Pfeiffer B, Winter K, Brehm W. Freeze-thaw cycles enhance decellularization of large tendons. Tissue Eng Part C Methods. 2014;20(4):276–284. doi:10.1089/ten.tec.2012.0760.
41. Qin TW, Chen Q, Sun YL, Steinmann SP, Amadio PC, An KN, Zhao C. Mechanical characteristics of native tendon slices for tissue engineering scaffold. J Biomed Mater Res B Appl Biomater. 2012;100(3):752–758. eng. doi:10.1002/jbm.b.32508.
42. Pfaffl MW. A new mathematical model for relative quantification in real-time RT-PCR. Nucleic Acids Res. 2001;29(9):e45. eng.

43. Rudin LI, Osher S, Fatemi E. Nonlinear total variation based noise removal algorithms. Physica D Nonlinear Phenomena. 1992;60(1):259–268. doi:10.1016/0167-2789(92)90242-F.
44. Gonzalez RC, Woods RE. Digital image processing prentice hall. 3 rd ed. Upper Saddle River, NJ: Prentice Hall International; 2002.
45. Jiang K, Wang Z, Du Q, Yu J, Wang A, Xiong Y. A new TGF-beta3 controlled-released chitosan scaffold for tissue engineering synovial sheath. J Biomed Mater Res A. 2014;102(3): 801–807. eng.
46. Moshaverinia A, Xu X, Chen C, Ansari S, Zadeh HH, Snead ML, Shi S. Application of stem cells derived from the periodontal ligament or gingival tissue sources for tendon tissue regeneration. Biomaterials. 2014;35(9):2642–2650. eng.
47. Durgam SS, Stewart AA, Pondenis HC, Gutierrez-Nibeyro SM, Evans RB, Stewart MC. Comparison of equine tendon- and bone marrow–derived cells cultured on tendon matrix with or without insulin-like growth factor-I supplementation. Am J Vet Res. 2012;73(1):153–161. doi:10.2460/ajvr.73.1.153.
48. Hao J, Zhang Y, Jing D, Shen Y, Tang G, Huang S, Zhao Z. Mechanobiology of mesenchymal stem cells: perspective into mechanical induction of MSC fate. Acta Biomater. 2015;20: 1–9. eng. doi:10.1016/j.actbio.2015.04.008.
49. Ingber DE. Tensegrity-based mechanosensing from macro to micro. Prog Biophys Mol Biol. 2008;97(2-3):163–179. eng. doi:10.1016/j.pbiomolbio.2008.02.005.
50. MacQueen L, Sun Y, Simmons CA. Mesenchymal stem cell mechanobiology and emerging experimental platforms. J R Soc Interface. 2013;10(84):20130179. eng. doi:10.1098/rsif.2013.0179.
51. Huebsch N, Arany PR, Mao AS, Shvartsman D, Ali OA, Bencherif SA, Rivera-Feliciano J, Mooney DJ. Harnessing traction-mediated manipulation of the cell/matrix interface to control stem-cell fate. Nat Mater. 2010;9(6):518–526. eng. doi:10.1038/nmat2732.
52. Ivaska J, Heino J. Cooperation between integrins and growth factor receptors in signaling and endocytosis. Annu Rev Cell Dev Biol. 2011;27:291–320. eng. doi:10.1146/annurev-cellbio-092910-154017.
53. Klein MB, Yalamanchi N, Pham H, Longaker MT, Chang J. Flexor tendon healing in vitro: Effects of TGF-beta on tendon cell collagen production. J Hand Surg Am. 2002;27(4): 615–620. eng.
54. Lu P, Zhang GR, Cai YZ, Heng BC, Ren H, Wang LL, Ji J, Zou XH, Ouyang HW. Lentiviral-encoded shRNA silencing of proteoglycan decorin enhances tendon repair and regeneration within a rat model. Cell Transplant. 2013;22(9):1507–1517. eng. doi:10.3727/096368912X661292.
55. Bottagisio M, Lopa S, Granata V, Talo G, Bazzocchi C, Moretti M, Lovati AB. Different combinations of growth factors for the tenogenic differentiation of bone marrow mesenchymal stem cells in monolayer culture and in fibrin-based three-dimensional constructs. Differentiation. 2017;95:44–53. eng. doi:10.1016/j.diff.2017.03.001.
56. Birk DE, Mayne R. Localization of collagen types I, III and V during tendon development. Changes in collagen types I and III are correlated with changes in fibril diameter. Eur J Cell Biol. 1997;72(4):352–361. eng.
57. Dowling BA, Dart AJ, Hodgson DR, Smith RK. Superficial digital flexor tendonitis in the horse. Equine Vet J. 2000;32(5): 369–378. eng.
58. Burk J, Gittel C, Heller S, Pfeiffer B, Paebst F, Ahrberg AB, Brehm W. Gene expression of tendon markers in mesenchymal stromal cells derived from different sources. BMC Res Notes. 2014;7(1):826. doi:10.1186/1756-0500-7-826.
59. Nakamura N, Hart DA, Boorman RS, Kaneda Y, Shrive NG, Marchuk LL, Shino K, Ochi T, Frank CB. Decorin antisense gene therapy improves functional healing of early rabbit ligament scar with enhanced collagen fibrillogenesis in vivo. J Orthop Res. 2000;18(4):517–523. eng. doi:10.1002/jor.1100180402.
60. Youngstrom DW, LaDow JE, Barrett JG. Tenogenesis of bone marrow-, adipose-, and tendon-derived stem cells in a dynamic bioreactor. Connect Tissue Res. 2016;57(6):454–465. eng. doi:10.3109/03008207.2015.1117458.
61. Youngstrom DW, Barrett JG, Jose RR, Kaplan DL. Functional characterization of detergent-decellularized equine tendon extracellular matrix for tissue engineering applications. Plos One. 2013;8(5):e64151. eng. doi:10.1371/journal.pone.0064151.
62. Gratzer PF, Harrison RD, Woods T. Matrix alteration and not residual sodium dodecyl sulfate cytotoxicity affects the cellular repopulation of a decellularized matrix. Tissue Eng. 2006; 12(10):2975–2983. eng. doi:10.1089/ten.2006.12.2975.
63. Schweitzer R, Chyung JH, Murtaugh LC, Brent AE, Rosen V, Olson EN, Lassar A, Tabin CJ. Analysis of the tendon cell fate using Scleraxis, a specific marker for tendons and ligaments. Development. 2001;128(19):3855–3866. eng.
64. Liu H, Zhu S, Zhang C, Lu P, Hu J, Yin Z, Ma Y, Chen X, OuYang H. Crucial transcription factors in tendon development and differentiation: their potential for tendon regeneration. Cell Tissue Res. 2014;356(2):287–298. eng. doi:10.1007/s00441-014-1834-8.
65. Kuo CK, Tuan RS. Mechanoactive tenogenic differentiation of human mesenchymal stem cells. Tissue Eng Part A. 2008;14(10):1615–1627. eng. doi:10.1089/ten.tea.2006.0415.
66. Liu J, Tao X, Chen L, Han W, Zhou Y, Tang K. CTGF positively regulates BMP12 induced tenogenic differentiation of tendon stem cells and signaling. Cell Physiol Biochem. 2015;35(5):1831–1845. eng. doi:10.1159/000373994.
67. Chamberlain CS, Lee JS, Leiferman EM, Maassen NX, Baer GS, Vanderby R, Murphy WL. Effects of BMP-12-releasing sutures on Achilles tendon healing. Tissue Eng Part A. 2015; 21(5-6):916–927. eng. doi:10.1089/ten.TEA.2014.0001.
68. Lou J, Tu Y, Burns M, Silva MJ, Manske P. BMP-12 gene transfer augmentation of lacerated tendon repair. J Orthop Res. 2001;19(6):1199–1202. doi:10.1016/S0736-0266(01)00042-0.
69. Derynck R, Zhang YE. Smad-dependent and Smad-independent pathways in TGF-beta family signalling. Nature. 2003;425(6958):577–584. eng. doi:10.1038/nature02006.